




Cite this: *RSC Adv.*, 2017, 7, 41727

# Unravelling diversity and metabolic potential of microbial consortia at each stage of leather sewage treatment†

Hebin Liang,<sup>ab</sup> Dongdong Ye<sup>ab</sup> and Lixin Luo <sup>\*ab</sup>

Activated sludge is essential for the biological wastewater treatment process and the identification of active microbes enlarges awareness of their ecological functions in this system. Microbial communities and their active members were investigated in activated sludge from a leather sewage treatment plant by a combined approach targeting both 16S rRNA and 16S rRNA genes. Although active bacteria obtained by RNA analysis exhibit similar diversity with DNA-based populations, the distribution of microbes significantly differed between the total and active communities. Several active taxa showed low abundance or even absence in the DNA-derived community. Moreover, microbial consortia, particularly bacterial communities, distinctly distributed at a particular treatment stage and both the total and active bacterial communities displayed high environmental sensitivity. Distributions of archaeal communities remained stable and the overrepresentations of active *Cenarchaeaceae* and *Nitrosopumilaceae* were potentially associated with ammonia oxidation across the treatment process. Furthermore, bacteria quantitatively dominate the microbial community in activated sludge and the 16S rRNA : 16S rRNA gene ratios of bacteria were positively correlated with the removal of contaminants. The results indicate that both dominant and low-abundance taxa with high potential activity play pivotal roles in removal of contaminants within sewage.

Received 6th July 2017  
 Accepted 19th August 2017

DOI: 10.1039/c7ra07470k

[rsc.li/rsc-advances](http://rsc.li/rsc-advances)

## 1. Introduction

In recent years, people around the world have increasingly focused on researching wastewater treatment. Wastewater, particularly industrial wastewater, leads to the decline of water quantity and quality and the leather industry is one of the most polluting industries in terms of the volume and the complexity of treatment of its effluents discharge.<sup>1</sup> Leather wastewater is considered as a severe pollutant source for the environment due to its high concentration of inorganic/organic matters, nitrogenous compounds, color content, variable pH together with total suspended solids.<sup>2,3</sup> Excess unqualified tannery wastewater can cause many deleterious effects, including the deterioration of ecological equilibrium.<sup>3</sup> Therefore, an efficient treatment before its discharge is essential for reducing the detrimental effects to the water environment.

Biological wastewater treatments are the most extensive pathway for wastewater treatment due to their low operational cost and high efficiency for contaminants removal.<sup>4</sup> Activated

sludge was composed of complex microbial consortia including bacteria, archaea, eukaryotes as well as viruses, in which bacteria are most dominant and play essential roles in biological treatment process.<sup>5</sup> Hence, detailed information on microbial communities and their interactions may provide new sights into the control of biological treatment process and will help in improvement of removal efficiency. Currently, high-throughput sequencing has been widely applied to analyze DNA-based microbial diversity and abundance in various samples, such as soil,<sup>6</sup> marine sediment<sup>7</sup> and activated sludge.<sup>8</sup> However, DNA associated with dead cells or the extent to residual “naked DNA” from cell lysis may mislead our acquaintances on microbial diversity and function in the environment.<sup>9</sup> Moreover, dormant microorganisms with a low metabolic state might also dissemble changes in the active microbes with important ecosystem function.<sup>10</sup> Although dormant cells can contain measurable numbers of ribosomes,<sup>11</sup> rRNA transcripts, compared to rRNA genes, would be more reliable in detection of active state within a given consortia<sup>12</sup> due to its higher concentration in active cells, since rRNA is a critical component of ribosomes which is essential to protein synthesis of growing cell.

Previous studies have assessed the total and active microbial communities in forest soil,<sup>13</sup> salt marsh sediments,<sup>10</sup> membrane bioreactor<sup>14</sup> and anaerobic digestion of pig slurry<sup>15</sup> by analysis of 16S rRNA gene and 16S rRNA, which further detected the active microbial community. However, most of the descriptive

<sup>a</sup>School of Bioscience and Bioengineering, South China University of Technology, Guangzhou, 510006, China. E-mail: [btlxluo@scut.edu.cn](mailto:btlxluo@scut.edu.cn); Fax: +86-20-39380601; Tel: +86-20-39380628

<sup>b</sup>Guangdong Provincial Key Laboratory of Fermentation and Enzyme Engineering, South China University of Technology, Guangzhou 510006, China

† Electronic supplementary information (ESI) available. See DOI: 10.1039/c7ra07470k



studies relies on sequence analysis targeting the 16S rRNA genes within activated sludge, which provides information regarding the total community of microbes (including active, dead and dormant individuals).<sup>7,8,16</sup> Nevertheless, still comparatively little is known about the dormant and active microbial communities at each stage of an integrated tannery wastewater treatment process and their responses to physicochemical parameters. Hence, the combination of investigation *via* DNA and RNA-based detection on microbial community may help us distinguish potentially active microbial cells from dead cells in treatment process and provide insights into the response of microbial communities, especially the active taxa with ecosystem function.

With the aid of high-throughput sequencing method, diversity and dynamics of microbial communities at each step in an integrated treatment process were well studied by DNA and RNA-based methods. Additionally, the abundances of total and potentially active populations of bacteria and archaea were appraised by means of qPCR and reverse transcription qPCR (RT-qPCR) targeting the 16S rRNA gene sequence. Multivariate analyses were performed to appraise the microbial dormancy and potential activity in the process and their responses to environmental conditions.

## 2. Material and methods

### 2.1. Samples collection

Mixed-liquor samples were taken from the homogeneous tank (HT), oxidation ditch (OD), influent of anoxic tank (AI), oxyc tank (OT), secondary oxyc tank (SOT) and effluent of secondary oxyc tank (SOE) of a full-scale industrial sewage treatment plant in Shangqiu City, Henan Province, China (34°25'N 115°39'E) which treats tannery wastewater (Fig. 1). This plant is designed to remove ammonium and inorganic/organic matter with the combination of oxidation ditch and anoxic/oxic/oxic (A/O/O) process. Three subsamples were collected and combined at each treatment step. Then, the samples were immediately delivered to the laboratory in ice box and stored in a -20 °C refrigerator for further usage.

Table 1 Characteristics of 7 mixed-liquor samples<sup>a</sup>

Sample	COD (mg L <sup>-1</sup> )	TAN (mg L <sup>-1</sup> )	pH
HT	1005.20	112.6 ± 10.53	8.21 ± 0.08
OD	149.05 ± 14.71	70.16 ± 6.35	8.07 ± 0.14
AI	184.51 ± 27.85	57.32 ± 7.19	8.22 ± 0.12
AT	117.2 ± 10.64	29.67 ± 6.14	8.02 ± 0.1
OT	109.66 ± 22.15	22.52 ± 5.35	8.08 ± 0.1
SOT	125.33 ± 25.1	13.58 ± 2.03	8.16 ± 0.08
SOE	118.36 ± 9.85	12.44 ± 3.38	8.19 ± 0.05

<sup>a</sup> Abbreviations: HT: homogeneous tank; OD: oxidation ditch; AI: anoxic tank influent; OT: oxyc tank; SOT: secondary oxyc tank; SOE: secondary oxyc tank effluent. COD: chemical oxygen demand; TAN: total ammonia nitrogen concentration.

### 2.2. Chemical analyses

For each sampling site, physicochemical characteristics and operational parameters were determined (Table 1). pH was measured in suit using STARTER 300 pH meter (Ohaus, USA). Chemical oxygen demand (COD) and total ammonium nitrogen were measured by the potassium dichromate method and Nessler's reagent spectrophotometry, respectively. Details of measurement and calculation were described as our previous study.<sup>17</sup>

### 2.3. Nucleic acids extraction, reverse transcription and illumina sequencing

For each mixed-liquor sample, samples of 20 ml were centrifuged at 8000 rpm. For 10 min at 4 °C to collect the activated sludge. Then DNA and RNA were extracted from the pellet with E.Z.N.A.® Soil DNA Kit and E.Z.N.A.® Soil RNA Kit (Omega Bio-Tek, Norcross, GA, USA) respectively according to the manufacturer's instructions.

The concentration and purity of RNA and DNA was determined by using NanoDrop 1000 Spectrophotometer (Thermo Fisher Scientific, USA). The erasure of genomic DNA and reverse transcription reactions were performed with PrimeScript™ RT reagent Kit with gDNA Eraser (Takara, Japan), following the manufacturer's protocol and using 2 µg RNA in a final volume of 60 µl. Both cDNA and DNA were stored at -80 °C for subsequent

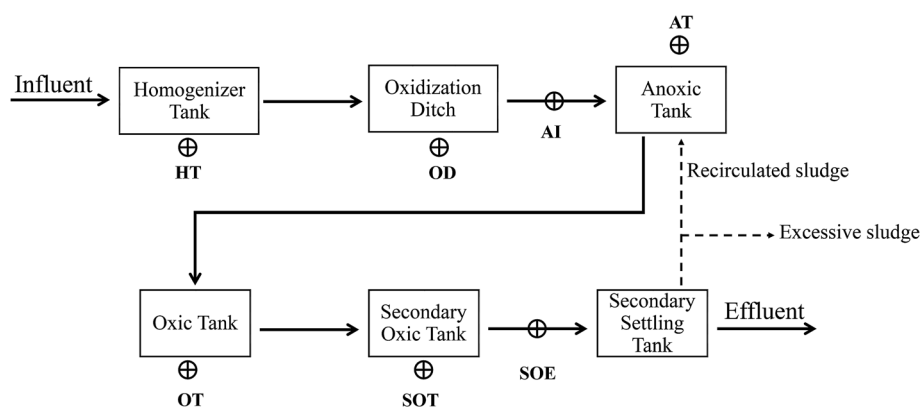


Fig. 1 Schematic diagram of the sewage treatment process and sampling points. Sampling points: HT: homogeneous tank; OD: oxidation ditch; AI: anoxic tank influent; OT: oxyc tank; SOT: secondary oxyc tank; SOE: secondary oxyc tank effluent.



analyses. Subsequently, the V4 regions of the 16S rRNA for bacteria (~250 nucleotides) and archaea (~380 nucleotides) were amplified in three independent PCR reactions, then purified PCR products were used to construct sequencing libraries and the libraries were finally sequenced on an Illumina HiSeq2500 platform (for details, see ESI S1†). All 16S rRNA sequences from high-throughput sequencing have been deposited into the NCBI short-reads archive database with accession number SRP076775.

#### 2.4. Real-time qPCR assay

All qPCR assays were performed on an ABI 7500 Real Time PCR System (Applied Biosystems). The copy numbers of 16S rRNA and 16S rRNA genes were estimated by using universal primer pair 338F/518R for bacteria and PARCH340f/519r for archaea.<sup>18,19</sup> More details on qPCR calibration curves and qPCR procedure (including correlation coefficients and efficiency of PCR amplification) are described in ESI S2.†

#### 2.5. Sequence and statistical analysis

The raw sequencing data were processed using the QIIME pipeline v1.7.0 to obtain the high-quality tags<sup>20</sup> and chimera checked using UCHIME algorithm<sup>21</sup> against the reference database (Gold database) to generate clean data. Then the effective tags from all samples were clustered into operational taxonomic units (OTUs) using Uparse v7.0.1001 (ref. 22) with 97% similarity. Taxonomy was assigned to the representative sequences using the RDP classifier and Greengenes Database v. May 2013.<sup>23</sup> The following diversity analyses were determined in QIIME (v1.7.0):  $\alpha$ -diversity (Shannon index, Simpson index and number of observed OTUs), principal coordinate analysis (PCoA) and cluster analysis based on weighted UniFrac. The R Studio version 3.2.3. software (<http://www.r-project.org>)<sup>24</sup> was used for statistical analysis. Permutational analysis of variance (PERMANOVA) based on Euclidean distances was performed with 9999 permutations to assess significant differences in community composition between DNA community and RNA community in the R “vegan” package.<sup>25</sup> The similarity of bacterial community between DNA and RNA community was further estimated by principal components analysis (PCA) using R “vegan” package. SIMPER analysis in PRIMER-E v5 (PRIMER-E Ltd, Ivybridge, UK) was applied to filter out phyla that contributed to 30% of dissimilarity between DNA-derived and RNA-derived community. Standard Mantel test was used to determine correlations between environmental factors and community composition (based on the relative abundance of phyla) with the R “vegan” package. Redundancy analysis was conducted to further analyze changes in the bacterial community under constraint of physico-chemical parameters with Canoco for Windows version 4.5 software. All statistical tests performed in this study were assumed to be significant at  $P$ -values  $\leq 0.05$ .

#### 2.6. Network analysis and functional predictions

A Spearman correlation-based network analysis was used to detect the correlations between bacterial phyla and

environmental parameters. The Spearman correlation was calculated in the R “Hmisc” package<sup>26</sup> and  $P$ -value adjustments for coefficients were performed using Benjamini–Hochberg false discovery rate.<sup>27</sup> Any bacterial taxa with occurrence in  $\leq 20\%$  samples and averaged abundance  $\leq 1\%$  (in total 16S rRNA/16S rRNA gene sequences of each sample) were excluded. Only strong and statistically significant correlations (Spearman’s coefficient  $\geq 0.7$  or  $\leq -0.7$ ; corrected  $P$ -value  $\leq 0.05$ ) were visualized in Cytoscape v 3.4.0.<sup>28</sup>

The functional contents of our bacterial community dataset were assessed based on 16S rRNA/rRNA gene sequencing data with Phylogenetic Investigation of Communities by Reconstruction of Unobserved States (PICRUSt), which is a bioinformatics tool that allows for the reconstruction of a metagenome by inference of gene content using 16S ribosomal DNA sequences.<sup>29</sup> For the analysis, based on the rarefied 16S sequences, the closed-reference OTUs were picked against the May 2013 Greengenes database using QIIME v 1.7 according to the online protocol, then the PICRUSt algorithm adjusted for the resulting OTUs and finally predicted functional genes, which were further classified into KEGG (Kyoto Encyclopedia of Genes and Genomes) orthologues according to the online protocol described by the developers (<http://picrust.github.com/picrust/tutorials/quickstart.html#quickstart-guide>).

## 3. Results and discussion

### 3.1. Diversity of microbial communities

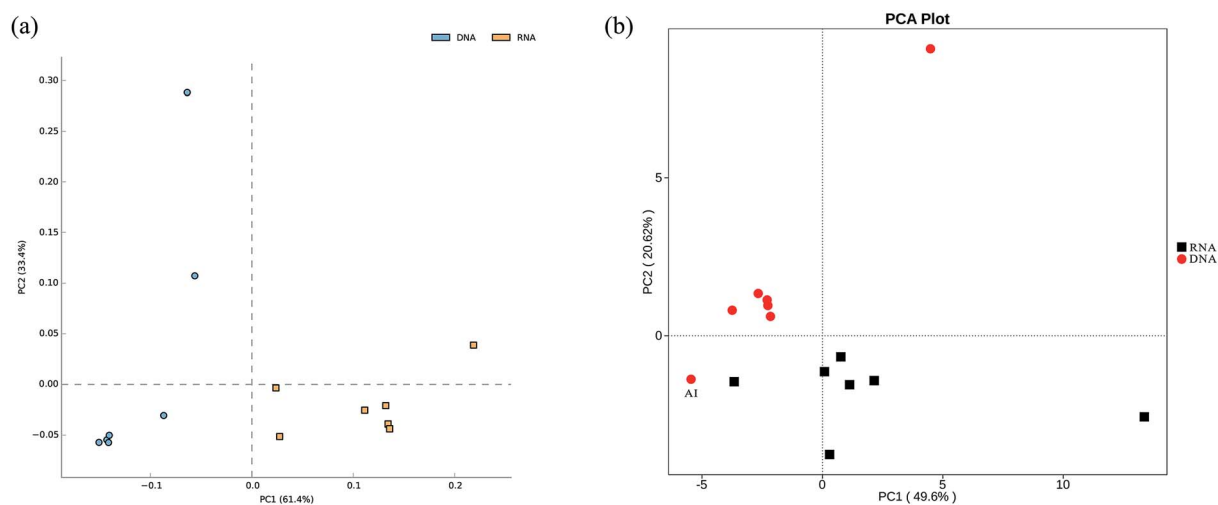
In total, approximately 721 680 sequence tags of bacterial 16S rRNA and 16S rRNA gene with an average length of 250 bp, and 709 919 tags of archaeal 16S rRNA and 16S rRNA gene with an average length of 380 bp were acquired after denoising and chimera removal. Following subsampling, a total of 26 664 and 16 477 OTUs, defined at 97% similarity for bacteria and archaea were obtained respectively.

To assess the internal (within-sample) complexity of individual microbial populations, the numbers of OTUs, Shannon and Simpson indices at cutoff level of 3% were summarized in Table 2. With regard to bacterial diversity, the Shannon and Simpson indices between total and active bacteria community showed no detectable distinctions (Table 2;  $P > 0.61$ ). Also, the Chao1 estimator predictions were not detectably different between total and active communities (Table 2;  $P > 0.8$ ). Strikingly, PCA followed by PERMANOVA showed significant differences in structure between total and active bacterial community (Fig. 2a,  $F = 13.14$ ,  $P < 0.001$ ), which was in line with previous studies in which the differences of microbial community structure between DNA- and RNA-derived communities had been reported.<sup>10,30,31</sup> A possible explanation for this observation was that DNA of some dead bacteria could persist for a prolonged period of time.<sup>9</sup> Furthermore, the divergence between the bacterial diversity and structure suggested that the structure of the active community cannot represent the total community, which was consistent with previous study.<sup>10</sup> Regarding the archaeal biodiversity, neither the diversity estimators (Chao1, Shannon and Simpson indices) nor structure were significantly different between



**Table 2** Diversity estimators of bacterial and archaeal communities based on OTU<sub>0.03</sub> obtained from high-throughput sequencing of DNA and RNA

Category	Sample	OTUs	Shannon	Simpson	Chao1	ACE	Goods coverage	
<b>Bacteria</b>								
DNA	HT	891	5.082	0.942	1414.44	1571.173	0.985	
	OD	1515	6.99	0.969	1472.267	1508.526	0.99	
	AI	1864	7.641	0.983	1776.667	1922.212	0.986	
	AT	2189	8.59	0.992	2381.439	2457.824	0.98	
	OT	2077	8.659	0.994	2260.65	2267.562	0.982	
	SOT	2134	8.435	0.991	2029.64	2104.107	0.984	
RNA	SOE	2118	8.693	0.993	2261.757	2313.769	0.982	
	HT	1494	5.076	0.905	1391.735	1512.119	0.992	
	OD	1860	7.219	0.975	1831.063	1876.748	0.992	
	AI	1819	7.562	0.986	1738.094	1783.152	0.992	
	AT	2113	7.926	0.987	2047.024	2085.496	0.992	
	OT	2140	7.764	0.982	2069.407	2126.919	0.991	
Archaea	SOT	2213	7.791	0.984	2141.347	2237.782	0.99	
	SOE	2237	8.587	0.993	2057.228	2133.893	0.994	
	DNA	HT	522	3.404	0.803	452.14	484.725	0.998
		OD	1208	6.692	0.943	1213.069	1206.356	0.995
		AI	1258	6.509	0.943	1238.283	1254.166	0.995
		AT	1424	7.052	0.961	1416.183	1446.092	0.994
OT		1340	6.664	0.94	1326.077	1350.274	0.995	
SOT		1353	6.717	0.942	1332.148	1343.893	0.995	
RNA	SOE	1345	6.848	0.946	1311.371	1335.742	0.996	
	HT	848	5.205	0.926	824.25	850.904	0.996	
	OD	1138	6.479	0.951	1089.121	1104.626	0.996	
	AI	1003	7.159	0.981	2106.81	1319.97	0.992	
	AT	1265	7.592	0.979	1250.519	1265.165	0.996	
	OT	1262	7.489	0.976	1280.685	1276.664	0.995	
SOT	1193	7.607	0.985	1190.986	1195.123	0.996		
SOE	1318	7.801	0.985	1287.785	1299.202	0.996		

**Fig. 2** Principal component analysis (PCA) plot showing both total and active bacterial communities (a), as well as their functional diversity (b).

DNA- and RNA-based archaeal community ( $P > 0.24$  and  $0.39$ , respectively; Table 2) which was in accordance with previous work in microbial electrolysis cells anode biofilm, indicating that the archaeal community within activated sludge was well depicted and kept certain stability in composition.<sup>15</sup>

Meanwhile, these results also indirectly validated the fact that eubacteria play a pivotal role in wastewater treatment.<sup>5</sup> In addition, the rarefaction curves tended to reach saturation, indicating that the sequencing depth could reveal the microbial diversity within these samples (Fig. S1†).



### 3.2. Differences between total and active microbial communities

**3.2.1. Relative abundance of bacterial community.** Altogether, a total of 45 bacterial phyla across all samples were identified (Fig. 3). *Proteobacteria* was the most dominant phylum in all samples, accounting for 43.3% and 57.98% to 49.48% and 76.74% of total and active effective bacterial tags, respectively and was followed by *Bacteroidetes* and *Firmicutes*, which was similar to previous reports.<sup>8,32</sup> However, the relative abundance of *Bacteroidetes* (8.21–14.82%, averaging at 10.5%) was slightly higher than that of *Firmicutes* (2.4–34.01%, averaging at 9.51%) at DNA level, while the opposite tendency was observed at RNA level (Fig. 3). Thus, distinguishing relationships between total and active microbial community provided insights into the potential shifts in activated sludge function which directly mediate the process performance, since activated sludge function was more likely related to the active community.<sup>10,33</sup> SIMPER analysis showed that *Proteobacteria*, *Firmicutes* and *Chloroflexi* severally contributed 35.3%, 12.96% and 9.9%

to the dissimilarity of total and active bacterial community (Fig. 3, Table S1†). Previous study has demonstrated that members of *Proteobacteria* possessed the ability in energy metabolism with reduced sulfur compounds and carbon assimilation *via* the reductive tricarboxylic acid (rTCA) cycle.<sup>34</sup> Consequently, the 21.2% overrepresentation in active *Proteobacteria* might be associated with the COD removal in sewage treatment process (Fig. 3, Table 1). Noteworthy, there were large differences in relative abundances of some phyla within total community (Fig. 3). For example, *Verrucomicrobia* was substantially more abundant in the sample from OD (9.22%), whereas *Firmicutes* was almost exclusively detected in the sample retrieved from HT (34.01%). This distinction might be linked to their adaptation to surrounding environmental variability.<sup>10</sup> Intriguingly, rare taxa (<1%), such as *Armatimonadetes*, [*Thermi*], *GAL15* and *NC10*, were preferentially detected in the RNA-based community (Fig S2†). The detection of *NC10* suggested their contribution to anaerobic methane oxidation coupled with denitrification during the treatment process.<sup>35</sup> At

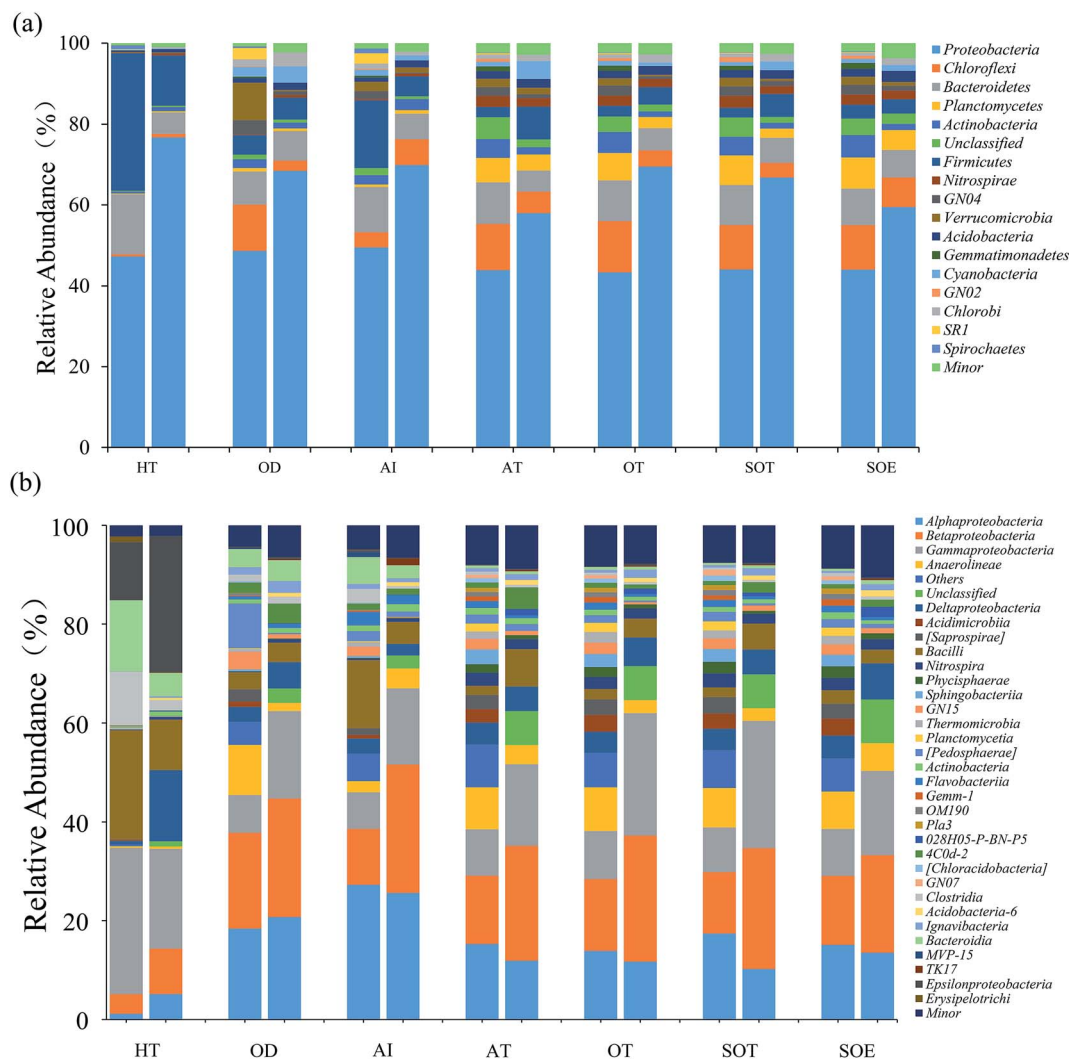


Fig. 3 Relative abundances of dominant bacterial taxa in both DNA communities (left column) and RNA communities (right column) for each sample: (a) phylum level (b) class level. Minor represents the taxa with abundance <1%.



class level, *Alphaproteobacteria*, *Betaproteobacteria* and *Gammaproteobacteria* were the predominant group in the total (15.48%, 12.81% and 11.73%, respectively) and active (14.11%, 21.76% and 19.60%, respectively) bacterial community, which was similar with previous study.<sup>8</sup> Strikingly, some classes including *Sphingobacteriia*, *GN15*, *Thermomicrobia*, *Planctomycetia*, and *Acidimicrobiia*, *Saprosirae* were detected over 1% share among the DNA bacterial communities, while they disappeared or appeared at low level in active bacterial populations (Fig. 3b). This could be explained by the residual DNA of the dead cells, low DNA concentration in cells and amplification biases.<sup>9,16,36</sup> The alternative interpretation for these differences might be the randomness of clone selection and the initial concentrations of the templates in the amplification reactions.<sup>37</sup> In addition, members of the genera *Sulfurospirillum*, *Acinetobacter*, *Arcobacter*, *Bacteroides* and *Aerococcus* were abundant in HT samples prior to other samples at both DNA and RNA level (Fig. S3 and S4†), whereas *Hyphomicrobium*, *Paracoccus*, *Nitrospira*, *Steroidobacter*, *Ignavibacterium*, *Azoarcus* and *Acinetobacter* appeared in five or more samples at both DNA and RNA level, indicating that the bacterial community evolved differently in the process was possibly due to the distinctive sewage characteristics and different operation parameters.<sup>38</sup> Although combined approaches targeting both 16S rDNA and 16S rRNA provided a more reliable description of total and active microbes than simple approaches,<sup>31</sup> the limitations of the

combined approaches could not be utterly negligible, since the rRNA concentration was not always linear with growing rate uniformly across taxa and therefore the relative rRNA abundance might not provide robust information regarding the potential activity of taxa.<sup>11</sup> Additionally, the copy number of ribosomal RNA operon (*rrn*) which typically codes for the 16S, 23S and 5S rRNAs differed significantly among taxa and was positively correlated with high translational power.<sup>39</sup> Thus, for the further utilization of rRNA data to characterize microbial communities, the relationships among these data, environmental conditions and community interactions should be better understood.<sup>11</sup>

### 3.2.2. Total and active archaeal community composition.

In case of archaeal community, phyla *Thaumarchaeota*, *Euryarchaeota* and *Crenarchaeota* were observed either in the DNA or the cDNA libraries among 7 samples, which was different from previous study in anaerobic digestion.<sup>40</sup> Yet, the predominant phylotype belonged to the archaeal family of *Cenarchaeaceae* (phylum *Thaumarchaeota*), representing on average  $77.3 \pm 6.77\%$  of total archaeal tags and the dominance was even stronger in the RNA-derived community (Fig. 4). Genomic analysis of *Cenarchaeum symbiosum* showed that this archaea harbored a number of homologues genes potentially associated with chemolithotrophic ammonia oxidation and thus might be involved in nitrogen cycling.<sup>41</sup> Also, in this work, *Cenarchaeum* was the most predominant genus in all samples and was

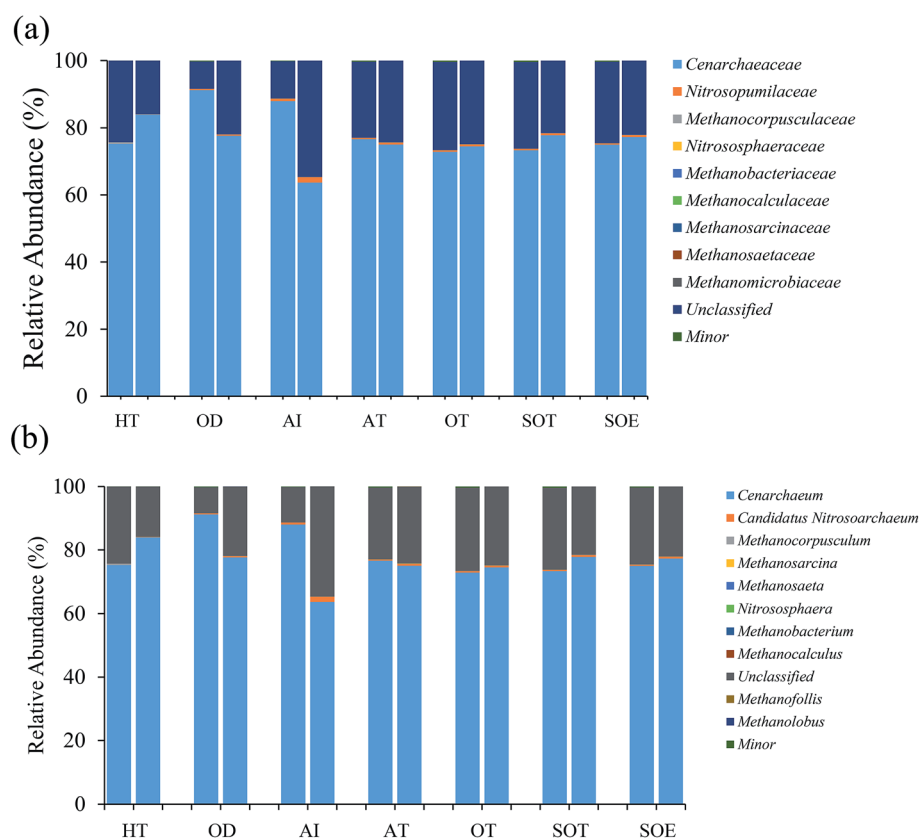


Fig. 4 Relative abundances of dominant archaeal taxa in both DNA communities (left column) and RNA communities (right column) for each sample: (a) family level (b) genus level. Minor represents the taxa with relative abundance <0.01%.



preferentially detected in the RNA, which indicates their activity during the treatment process. Furthermore, the *Nitrosopumilaceae*, which could oxidize ammonia in the absence of organic carbon,<sup>42</sup> was overrepresented by a 0.25% increase in relative abundance in the cDNA data set compared to the DNA data set, suggesting their potential activity in ammonia removal during this process. Nevertheless, no significant distinctions were observed between the total and active archaeal community (Fig. 4,  $P > 0.39$ ), possibly due to the high proportion of *Cenarchaeaceae*. Additionally, *Methanocorpusculaceae*, *Methanocalculaceae* in DNA library and *Nitrososphaeraceae* in RNA library disappeared in one or two samples, which might reflect the evolution of microbes during the process. Noteworthy, *Methanocorpusculum* and *Methanobacterium* were detected in more than three samples (Fig. 4b), however, they disappeared in active populations and new genera including *Methanosarcina* and *Methanosaeta*, occurred, despite their low relative abundance in the 16S rRNA amplicon reads, which most likely be explained by the fact that the number of ribosome were much higher in active cells than that in dormant cells.<sup>43</sup> Previous studies demonstrated that *Methanosaeta*, a methanogenic archaea exclusively conducting acetoclastic methanogenesis, was negatively correlated with the total ammonium nitrogen

concentration and kept increased activity under high organic acids concentrations,<sup>44,45</sup> which was in line with the increase in the relative abundance of *Methanosaeta* and the decline of total ammonium nitrogen concentration in the present study (Fig. 4b, Table 1). Therefore, the occurrence of *Methanosaeta* might contribute to the methanogenesis among the process. Additionally, *Methanosarcina* was preferentially detected in the sample from AT, which was consistent with the results in anaerobic digestion (Fig. 4b).<sup>45</sup>

### 3.3. Environment-species associations and functional prediction

Environmental factors are generally considered as critical roles for changes of microbial consortia in activated sludge.<sup>30</sup> In this study, multivariate analyses were applied to detect this relationship. The Mantel test indicated significant correlations ( $r = 0.704$ ,  $P = 0.022$ ) between DNA-derived bacterial assemblages and physicochemical variables, which displayed tighter than that of RNA community ( $r = 0.6208$ ,  $P = 0.032$ ). This is in line with the previous study in activated sludge.<sup>38</sup> Moreover, RDA analysis and the integrated network analysis further confirmed this and revealed the environment-species associations (Fig. 5). Ecological functions could be associated with 81.87–98.87% of

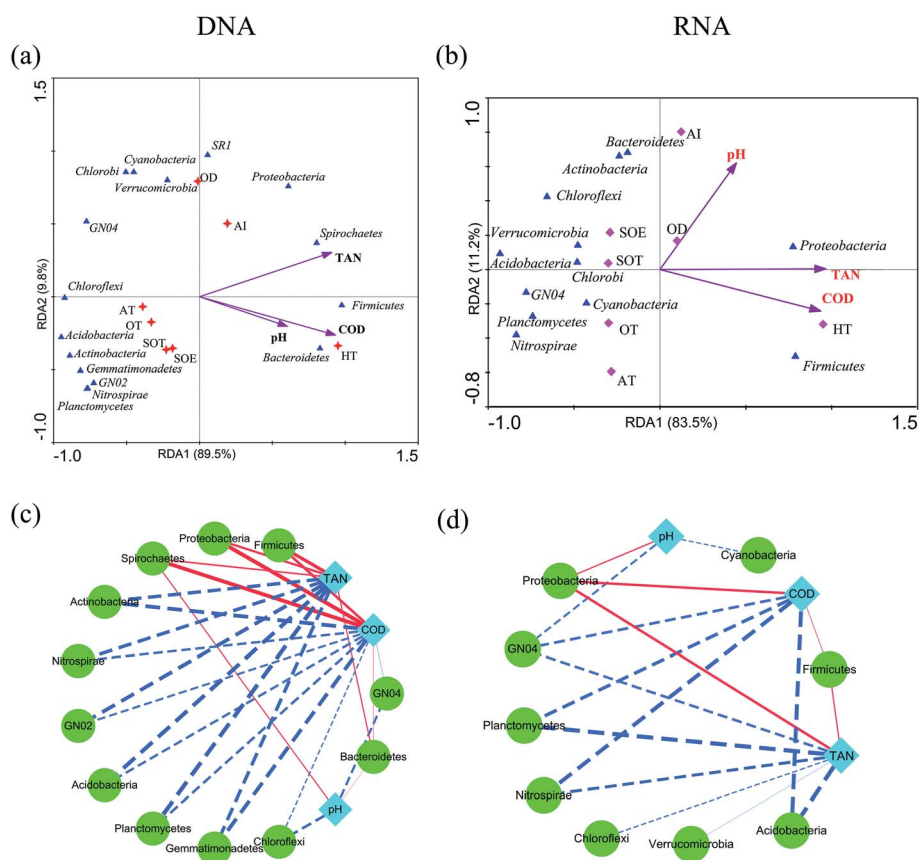


Fig. 5 RDA and network analyses of bacterial community. Only Spearman's correlation coefficient that were statistically significant (corrected  $P < 0.05$ ) are shown in the network. Nodes represent a bacterial phylotype (green color) or environmental factor (cyan color). The dashed line in red indicates negative correlation and the solid line indicates positive correlation. The line thickness is proportional to the absolute value of Spearman's correlation coefficient. TAN: total ammonium nitrogen.



the dominant phyla of the bacterial community. Among the selected phyla, such as *Proteobacteria*, *Bacteroidetes*, *Firmicutes* and *Spirochaetes*, relative abundance in the DNA community was primarily correlated with COD and total ammonium nitrogen *via* positive correlations (Fig. 5a). Thus, the increase in COD and total ammonium nitrogen concentration may result in the accumulation of these phyla, by contrast, negative correlations dominated the associations between COD, total ammonium nitrogen and bacterial taxa, meaning that the increase in COD and total ammonium nitrogen may reduce the abundance of most dominant phyla in wastewater treatment process. Regarding the RNA community, *Proteobacteria* was strongly positive with COD and total ammonium nitrogen concentration (Spearman correlation: COD,  $\rho = 0.853$ ,  $P = 0.0003$ ; total ammonium nitrogen,  $\rho = 0.863$ ,  $P = 0.0002$ , respectively) and *Firmicutes* showed the similar correlation (COD,  $\rho = 0.744$ ,  $P = 0.004$ ; total ammonium nitrogen,  $\rho = 0.78$ ,  $P = 0.002$ , respectively), while all the rest presented negative correlations with COD and total ammonium nitrogen concentration (Fig. 5b,  $P < 0.05$ ). Indeed, network analysis (Fig. 5c and d) further tracked that COD and total ammonium nitrogen with more edges related to bacterial phyla explained much better association with bacterial diversity than pH with fewer edges,

indicating that COD and total ammonium nitrogen in this process may significantly influence the microbial structure, as described elsewhere.<sup>17,38</sup> Positive correlations between active *Proteobacteria* and COD could potentially contribute to its overrepresentation compared to the total community.<sup>34</sup> Moreover, *Nitrospira*, who was considered as nitrite-oxidizing bacteria, had a negative relationship with total ammonium nitrogen concentration, which could be transformed to nitrite by ammonia-oxidizing bacteria.<sup>38</sup> Thus, the increase in *Nitrospira* abundance within both total and active community could be linked with the reduction of total ammonium nitrogen concentration. Previous study reported that *Acidobacteria* was capable of competing substrate *via* K-selected strategy.<sup>46</sup> Indeed, in this work, phylum *Acidobacteria* was negatively related with COD concentration and was preferentially detected in the RNA-based community, which indicated their activity during the process. In addition, there was no significant effect of pH on total and active community structure (Fig. 5a and b,  $P > 0.42$ ), which could be interpreted by the stability of pH (Table 1). However, no significant linkages were observed between environmental variability and archaeal community composition in either DNA samples or RNA samples ( $P > 0.05$ ), which might result from the insignificant variation of archaeal

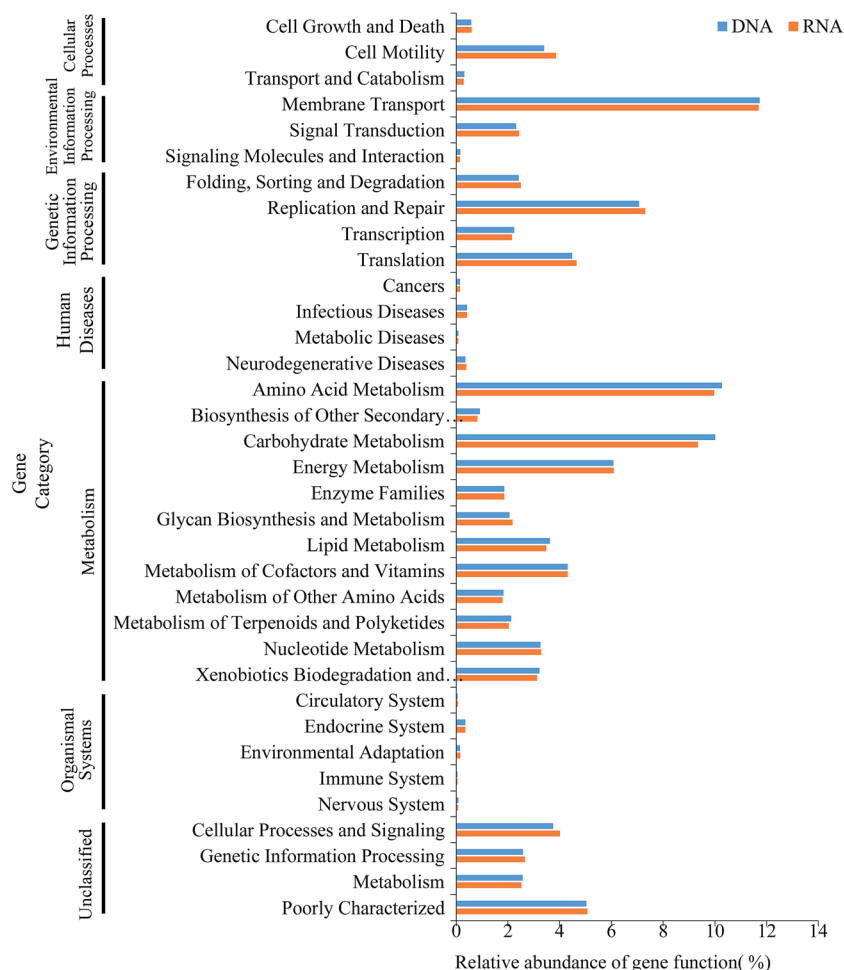


Fig. 6 Comparison of predicted metabolic functions of the DNA- and RNA-based bacterial communities found in activated sludge.



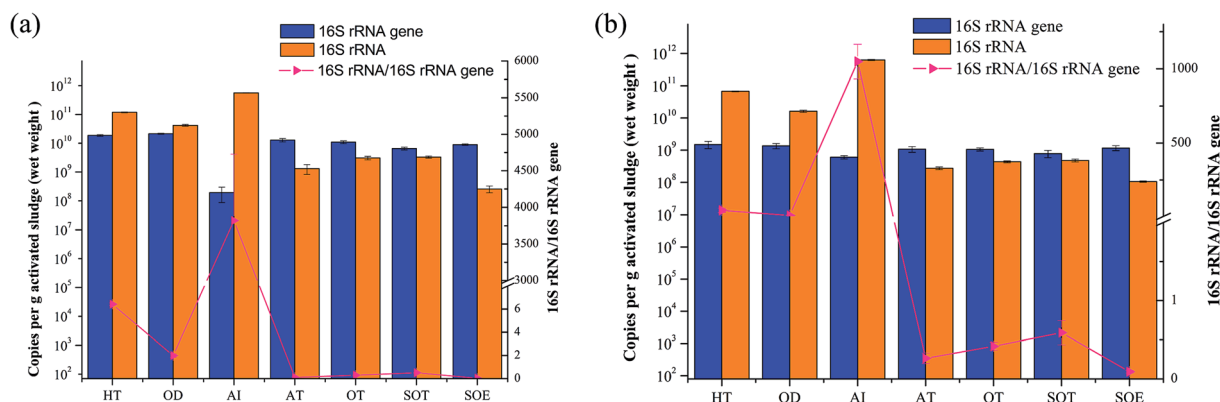


Fig. 7 Quantification of the relative abundance of microbial 16S rRNA genes and their transcripts in 7 samples. (a) Bacteria; (b) archaea.

community structure. Overall, the environment-species associations in this study preliminarily implicated the importance of same environmental filters in shaping assembly of both total and active bacterial communities in activated sludge.<sup>30,38</sup>

The microbial consortia within activated sludge may manifest many crucial functions which are essential to biological wastewater treatment. In present study, PICRUSt, a predictive exploratory tool, was performed to predict metabolic functions of bacterial 16S rRNA/rRNA genes and found that 41 level 2 KEGG orthology groups which might be associated with variations in OTU abundance detected *via* 16S sequencing were inferred in the activated sludge. The predictive functional profiling (Fig. 6) indicated that the most predicted metabolic functional categories were related to membrane transport (11.25–12.8%), amino acid metabolism (9.18–10.48%), carbohydrate metabolism (8.51–10.12%), replication and repair (6.87–7.96%) and energy metabolism (5.8–6.74%), suggesting that microbes in activated sludge kept metabolically active during the process, which in accordance with the conventional interpretation that the complex mixture of pollutant within wastewater were degraded by a diverse metabolic pathways of cells.<sup>47</sup> When comparing the function of gene predicated with the active bacteria of the complete bacterial community, the relative abundances of most of the gene families of DNA community showed significantly statistical differences with that of RNA community (Fig. 2b,  $F = 3.41$ ,  $P = 0.0142$ ). However, the bacterial 16S rRNA genes from AI showed no significant statistical differences in predictive functional profiling with bacterial 16S rRNA, which could be interpreted the inherent limitation that the accuracy of PICRUSt is dependent on the phylogenetic dissimilarity among reference genomes and sequenced sequence.<sup>29</sup> An alternative explanation might be the loss of those genes which were not included in the input database.<sup>29</sup> Unfortunately, we also found genes relating to human disease in those samples, which was in line with the aforementioned detections of *Clostridium* and *Arcobacter* (Fig. S3 and S4†).<sup>48,49</sup> Even though several functions were inferred by PICRUSt, the loss of many actual functions of microbe in activated sludge should be further explored with the aid of multiple omics approaches.

### 3.4. Quantifications and 16 rRNA/rRNA gene ratios of total bacteria and archaea

Synchronously quantifying the number of copies of the 16S rRNA and 16S rRNA genes in the same set of assays provided new insights into both the abundances and activity status of the microbial communities. Fig. 7 showed the mean copies of 16S rRNA genes and 16S rRNA of both bacteria and archaea. The results indicated that the abundance of total bacterial and archaeal were slightly variable throughout the integrated treatment process, while the values of copy numbers of bacterial and archaeal 16S rRNA were 1–3 orders of magnitude in HT, OD and AI than other samples. Additionally, the 16S rRNA genes copy numbers of bacteria were higher than those of archaea, indicating that bacteria played an important role in biological wastewater treatment.<sup>5</sup>

The 16S rRNA/16S rRNA gene ratio was frequently applied to estimate microbial activity and the 16S rRNA/16S rRNA gene ratio  $> 1$  was considered as a threshold for whether the microbe was potentially active to assess the diversity of active taxa.<sup>10,16,50</sup> Previous study reported that metabolically active *Mycolata* with high 16S rRNA/16S rRNA gene ratio might lead to foaming in membrane bioreactors (MBRs).<sup>50</sup> In this study, the 16S rRNA/16S rRNA gene ratio ranged from 1.96 to 2907.35 across samples from HT, OD and AI in both bacterial and archaeal communities, suggesting that microbes in these samples kept potentially metabolic activity. However, the ratios sharply decreased to less than one in the later stage, especially the 16S rRNA/16S rRNA gene ratio in sample from SOE which almost went down to 0, presuming that it contained on average less active populations than other samples, possibly due to the nutrient limitation (Table 1). Hence, we concluded that both the higher rRNA concentrations and 16S rRNA/16S rRNA gene ratios indirectly reflected the relationship between potentially metabolic activity of microbes and nutrient, as well as the removal efficiency.

## 4. Conclusions

In this work, microbial community and its active taxa were compared in activated sludge by the independent analysis of



16S rRNA and 16S rRNA gene. The results demonstrated that the active community significantly differed from the total community. The dominant group, such as *Proteobacteria*, and rare taxa with low abundance, such as *NC10* and *GAL15*, were preferentially detected in the RNA-based community, indicating the limitations of DNA-based study, which possibly miss considerable portions of active microbial populations. In the activated sludge, microbial communities showed differences in their distributions due to the characteristics of wastewater and the 16S rRNA/16S rRNA gene ratio of microbes presented a downward trend along with the process, which likely result from nutrition deficiency. Thus, environmental factors could affect both total and active communities within activated sludge. Further study should focus on the relationships between total and active communities and how environmental change influences the associations to determine microbial function during wastewater treatment process.

## Conflicts of interest

The authors declare no conflict of interest.

## Acknowledgements

We would like to acknowledge the National Natural Foundation of China (grant 31271924) for the financial support. The authors would like to thank the lab colleagues for their endless support.

## References

- 1 A. Deghles and U. Kurt, *Chem. Eng. Process.*, 2016, **104**, 43–50.
- 2 A. Deghles and U. Kurt, *Desalin. Water Treat.*, 2016, **57**, 14798–14809.
- 3 R. Ganesh, P. Sousbie, M. Torrijos, N. Bernet and R. A. Ramanujam, *Clean Technol. Environ.*, 2015, **17**, 735–745.
- 4 L. Ye and T. Zhang, *Appl. Microbiol. Biotechnol.*, 2013, **97**, 2681–2690.
- 5 T. C. Yadav, A. A. Khardenavis and A. Kapley, *Bioresour. Technol.*, 2014, **165**, 257–264.
- 6 S. Banerjee, M. Baah-Acheamfour, C. N. Carlyle, A. Bissett, A. E. Richardson, T. Siddique, E. W. Bork and S. X. Chang, *Environ. Microbiol.*, 2016, **18**, 1805–1816.
- 7 J. Gong, F. Shi, B. Ma, J. Dong, M. Pachiadaki, X. Zhang and V. P. Edgcomb, *Environ. Microbiol.*, 2015, **17**, 3722–3737.
- 8 T. Zhang, M.-F. Shao and L. Ye, *ISME J.*, 2012, **6**, 1137–1147.
- 9 V. Kapoor, T. Pitkänen, H. Ryu, M. Elk, D. Wendell and J. W. Santo Domingo, *Appl. Environ. Microbiol.*, 2015, **81**, 91–99.
- 10 P. J. Kearns, J. H. Angell, E. M. Howard, L. A. Deegan, R. H. R. Stanley and J. L. Bowen, *Nat. Commun.*, 2016, **7**, 12881.
- 11 S. J. Blazewicz, R. L. Barnard, R. A. Daly and M. K. Firestone, *ISME J.*, 2013, **7**, 2061–2068.
- 12 R. C. Mueller, L. Gallegos-Graves, D. R. Zak and C. R. Kuske, *Microb. Ecol.*, 2016, **71**, 57–67.
- 13 P. Baldrian, M. Kolařík, M. Štursová, J. Kopecký, V. Valášková, T. Větrovský, L. Žifčáková, J. Šnajdr, J. Řídl and Č. Vlček, *ISME J.*, 2012, **6**, 248–258.
- 14 P. Maza-Márquez, R. Vilchez-Vargas, F.-M. Kerckhof, E. Aranda, J. González-López and B. Rodelas, *Water Res.*, 2016, **105**, 507–519.
- 15 M. Cerrillo, M. Viñas and A. Bonmatí, *Water Res.*, 2017, **110**, 192–201.
- 16 A. M. Klein, B. J. M. Bohannan, D. A. Jaffe, D. A. Levin and J. L. Green, *Front. Microbiol.*, 2016, **7**, 772.
- 17 H. Liang, D. Ye, P. Li, T. Su, J. Wu and L. Luo, *RSC Adv.*, 2016, **6**, 87380–87388.
- 18 G. Muyzer, E. C. De Waal and A. G. Uitterlinden, *Appl. Environ. Microbiol.*, 1993, **59**, 695–700.
- 19 L. Ovreås, L. Forney, F. L. Daae and V. Torsvik, *Appl. Environ. Microbiol.*, 1997, **63**, 3367–3373.
- 20 J. G. Caporaso, J. Kuczynski, J. Stombaugh, K. Bittinger, F. D. Bushman, E. K. Costello, N. Fierer, A. G. Pena, J. K. Goodrich and J. I. Gordon, *Nat. Methods*, 2010, **7**, 335–336.
- 21 R. C. Edgar, B. J. Haas, J. C. Clemente, C. Quince and R. Knight, *Bioinformatics*, 2011, **27**, 2194–2200.
- 22 R. C. Edgar, *Nat. Methods*, 2013, **10**, 996–998.
- 23 D. McDonald, M. N. Price, J. Goodrich, E. P. Nawrocki, T. Z. DeSantis, A. Probst, G. L. Andersen, R. Knight and P. Hugenholtz, *ISME J.*, 2012, **6**, 610–618.
- 24 R. C. Team, 2013, ISBN 3-900051-07-0, <http://www.R-project.org>.
- 25 J. Oksanen, F. G. Blanchet, R. Kindt, P. Legendre, P. R. Minchin, R. B. O'Hara, G. L. Simpson, P. Solymos, M. H. H. Stevens and H. Wagner, *Vegan: community ecology package, R package version 2.3-5*, 2016.
- 26 F. E. Harrell, R package version, 2008, 3, 4.
- 27 Y. Benjamini and Y. Hochberg, *J. R. Stat. Soc. Series B Stat. Methodol.*, 1995, 289–300.
- 28 P. Shannon, A. Markiel, O. Ozier, N. S. Baliga, J. T. Wang, D. Ramage, N. Amin, B. Schwikowski and T. Ideker, *Genome Res.*, 2003, **13**, 2498–2504.
- 29 M. G. Langille, J. Zaneveld, J. G. Caporaso, D. McDonald, D. Knights, J. A. Reyes, J. C. Clemente, D. E. Burkepille, R. L. V. Thurber and R. Knight, *Nat. Biotechnol.*, 2013, **31**, 814–821.
- 30 Y. Zhang, Z. Zhao, M. Dai, N. Jiao and G. J. Herndl, *Mol. Ecol.*, 2014, **23**, 2260–2274.
- 31 A. Rodríguez-Blanco, V. Antoine, E. Pelletier, D. Delille and J. F. Ghiglione, *Environ. Pollut.*, 2010, **158**, 663–673.
- 32 D. Shu, Y. He, H. Yue and Q. Wang, *Bioresour. Technol.*, 2015, **186**, 163–172.
- 33 K. J. Romanowicz, Z. B. Freedman, R. A. Upchurch, W. A. Argiroff and D. R. Zak, *FEMS Microbiol. Ecol.*, 2016, **92**, fiw149.
- 34 K. Takai, B. J. Campbell, S. C. Cary, M. Suzuki, H. Oida, T. Nunoura, H. Hirayama, S. Nakagawa, Y. Suzuki and F. Inagaki, *Appl. Environ. Microbiol.*, 2005, **71**, 7310–7320.
- 35 K. F. Ettwig, T. Van Alen, K. T. van de Pas-Schoonen, M. S. Jetten and M. Strous, *Appl. Environ. Microbiol.*, 2009, **75**, 3656–3662.



- 36 E. M. Fykse, T. Aarskaug, E. H. Madslie and M. Dybwad, *Bioresour. Technol.*, 2016, **222**, 380–387.
- 37 B. Nogales, E. R. B. Moore, E. Lobet-Brossa, R. Rossello-Mora, R. Amann and K. N. Timmis, *Appl. Environ. Microbiol.*, 2001, **67**, 1874–1884.
- 38 F. Ju and T. Zhang, *ISME J.*, 2015, **9**, 683–695.
- 39 S. F. Stoddard, B. J. Smith, R. Hein, B. R. Roller and T. M. Schmidt, *Nucleic Acids Res.*, 2014, **43**, D593–D598.
- 40 B. Lee, J.-G. Park, W.-B. Shin, D.-J. Tian and H.-B. Jun, *Bioresour. Technol.*, 2017, **234**, 273–280.
- 41 S. J. Hallam, K. T. Konstantinidis, N. Putnam, C. Schleper, Y.-i. Watanabe, J. Sugahara, C. Preston, J. de la Torre, P. M. Richardson and E. F. DeLong, *Proc. Natl. Acad. Sci. U. S. A.*, 2006, **103**, 18296–18301.
- 42 M. Könneke, A. E. Bernhard, R. José, C. B. Walker, J. B. Waterbury and D. A. Stahl, *Nature*, 2005, **437**, 543–546.
- 43 F. Fegatella, J. Lim, S. Kjelleberg and R. Cavicchioli, *Appl. Environ. Microbiol.*, 1998, **64**, 4433–4438.
- 44 A. M. Ziganshin, E. E. Ziganshina, S. Kleinsteuber and M. Nikolausz, *Archaea*, 2016, **2016**, 12.
- 45 A. M. Ziganshin, T. Schmidt, Z. Lv, J. Liebetrau, H. H. Richnow, S. Kleinsteuber and M. Nikolausz, *Bioresour. Technol.*, 2016, **217**, 62–71.
- 46 V. Torsvik and L. Øvreås, *Curr. Opin. Microbiol.*, 2002, **5**, 240–245.
- 47 E. W. Low and H. A. Chase, *Water Res.*, 1999, **33**, 1119–1132.
- 48 M. Sebahia, B. W. Wren, P. Mullany, N. F. Fairweather, N. Minton, R. Stabler, N. R. Thomson, A. P. Roberts, A. M. Cerdeño-Tárraga and H. Wang, *Nat. Genet.*, 2006, **38**, 779–786.
- 49 C. Phillips, *Food Control*, 2001, **12**, 1–6.
- 50 P. Maza-Márquez, R. Vilchez-Vargas, N. Boon, J. González-López, M. V. Martínez-Toledo and B. Rodelas, *Water Res.*, 2016, **92**, 208–217.

